Silica-Magnetite Composite as an Eco-Friendly Adsorbent for Aqueous Tetracycline Removal – Kinetic and Isotherm Studies

Sofyatuddin Karina[1,3], Adli Waliul Perdana[2,3], Vicky Prajaputra[1,3,4*],
Nadia Isnaini[3,4,5], Putri Hayyatun Nuufus[1], Audia Bismi[1]

[1] Department of Marine Sciences, Faculty of Marine and Fisheries, Universitas Syiah Kuala, Banda Aceh 23111, Indonesia

[2] Department of Aquaculture, Faculty of Marine and Fisheries, Universitas Syiah Kuala, Banda Aceh 23111, Indonesia

[3] Research Centre for Marine Sciences and Fisheries, Universitas Syiah Kuala, Banda Aceh 23111, Indonesia

[4] ARC-PUI PT Nilam Aceh, Universitas Syiah Kuala, Banda Aceh 23111, Indonesia

[5] Department of Pharmacy, Faculty of Mathematics and Natural Sciences, Universitas Syiah Kuala, Banda Aceh 23111, Indonesia

* Corresponding author e-mail's: vicky_prajaputra@usk.ac.id

ABSTRACT

Silica and magnetite have been recognized as emerging and effective environmentally-friendly pollutant removers. In this study, the effectiveness of silica/magnetite (SM) composites derived from local beach sand were developed and evaluated as an environmentally friendly adsorbent for taking up tetracycline from water. The formation of SM composites was verified through characterization performed using Fourier-transform infrared (FT-IR) spectroscopy, X-ray diffraction (XRD), and Scanning Electron Microscope (SEM) analysis. Two key parameters, kinetics and isotherms, were investigated to find the best condition for tetracycline adsorption using SM composites. In the kinetic adsorption studies, the pseudo-first-order, with correlation coefficients ($R^2 > 0.99$) higher than those of the pseudo-second-order and Elovich models, was performed to be the best-fitting model due to the close alignment between the experimental and theoretical data. The non-linear Langmuir isotherm model offered the most accurate fit ($R^2 = 0.954$, root-mean-square-errors = 1.505) compared to the Freundlich model, signifying that the adsorption process takes place on a uniform surface where the adsorbate is distributed in monolayers. In the present study, the maximum adsorption capacity of tetracycline onto SM composite reached 29.955 ± 4.165 mg/g for 24-hour contact time with an adsorption rate constant of 0.415 ± 0.050 min^{-1}. In conclusion, the developed environmentally conscious composite demonstrates the potential to be an effective adsorbent with remarkable tetracycline removal properties while also providing valuable insights for further research.

Keywords: adsorption, beach sand, degradation, silica magnetite composite, tetracycline.

INTRODUCTION

Tetracycline antibiotics find widespread use in aquaculture as an essential tool for maintaining the health and well-being of farmed aquatic species (Salma et al., 2023). These antibiotics are administered to fish and other aquatic organisms to prevent and treat bacterial infections, ensuring their overall health and growth (Rajeev et al., 2021). In aquaculture settings, tetracyclines are frequently added in feeding media as growth promoters to stimulate appetite and accelerate growth (Rigos et al., 2021). In the end, the use of tetracyclines becomes out of control, leading to an increase in the concentration of antibiotic residues in aquaculture waters. These residues can be released the aquatic environment when replacing the water from aquaculture, causing fish degenerative illnesses, algae

growth inhibition, and antibiotic-resistant bacteria (Yun et al., 2023; Le et al., 2023; Li et al., 2023). A study by Chang et al. (2023) has reported the presence of tetracycline residues in lake, river and marine sediments with the concentration of 0.196 mg/L, 0.422 mg/L, and 1.478 mg/L, respectively. Hence, it is imperative to implement a good method to address the issue of limited efforts in managing tetracyclines or other antibiotics contamination from water.

Adsorption has become one of the most cost-effective and easily implemented methods to reduce various levels of organic pollutants in wastewater due to its high effectiveness (Qiu et al., 2022; Ghosh et al., 2023). Organic compounds are adsorbed and accumulate on the surface of adsorbent particles as a result of interactions on the active surface sites. The surface area, the number of active surface sites of the adsorbent, and their accessibility greatly determine the effectiveness of the adsorption process (Prasetya et al., 2023). Various adsorbents have been used in the adsorption process, such as activated carbon (Sarker et al., 2023), zeolite (Prajaputra et al., 2019), pumice (Prajaputra et al., 2021; Prajaputra and Isnaini, 2023), chitosan (Said et al., 2023), clay (Ewis et al., 2022), fly ash (Behrami et al., 2022), and other natural materials or biomass (Amaly et al., 2022; De Mastro et al., 2022). To date, many researchers have focused on the development of locally sourced adsorbents that are both cost-effective and readily available.

Beach sand emerges as a promising natural resource for the production of potential adsorbent materials. The main component of beach sand is typically composed of finely ground mineral particles, primarily consisting of quartz (Chapkanski et al., 2022). Quartz is a crystalline form of silicon dioxide (SiO_2) and is renowned for its hardness, durability, and inert nature (Kumaravel et al., 2022). The silica extracted from beach sand presents a promising avenue for antibiotic adsorption applications. Its natural abundance and unique properties, including its high surface area, porosity, and abundant surface silanol (Si-OH) groups, make it an excellent adsorbent for the removal of antibiotics from aqueous solutions (Saxena et al., 2020; Zeidman et al., 2020). With the increasing concern about the presence of antibiotics in aquatic environments and the potential for antibiotic resistance development, utilizing beach sand-derived silica as an adsorbent offers an eco-friendly and effective solution. However, one notable weakness of silica as an adsorbent is its challenging separation process after adsorption. In the present study, significant improvements were made by incorporating silica with magnetite, imparting magnetic properties to the adsorbent. This innovative approach allows for the easy separation of the adsorbent from the treated solution using a simple magnetic rod after the adsorption process. Tetracycline was selected as the model organic compound for adsorption, serving as a representative example of pharmaceutical contaminants in water. To the best of authors' knowledge, this research represents the inaugural investigation into the fabrication of silica/magnetite composites sourced from beach sand as a raw material, and their subsequent application as an adsorbent for tetracycline removal from water. The objective of this study was to assess the potential of a silica/magnetite composite as an efficient and environmentally friendly adsorbent for the removal of tetracycline from aqueous solutions. To achieve this goal, a series of adsorption studies was conducted, systematically varying key operational factors including contact time, adsorbent dosage, and initial tetracycline concentration. The adsorption kinetics were analyzed using pseudo-first-order, pseudo-second-order, and Temkin models, while the equilibrium data were scrutinized and modeled using Langmuir as well as Freundlich isothermal models.

MATERIAL AND METHODS

The present study was carried out within the marine chemistry and biotechnology laboratory, located in the Faculty of Marine and Fisheries at Universitas Syiah Kuala. Beach sand samples were collected from two locations in the Aceh Besar area, namely Lhok Mee Beach and Leungah Beach. The two locations were selected because of the high amount of silica and iron contents in the beach sand at those places. The sand samples were collected from a depth approximately 30 centimetres above the beach surface using a PVC pipe of 3 inches in diameter. The collected samples were washed with distilled water, dried at 100°C, and ground into a powder before being employed as raw materials for preparing silica/magnetite composites. The high-quality reagents utilized in this experiment were all purchased from Merck. These reagents included tetracycline ($C_{22}H_{24}N_2O_8$), sodium hydroxide (NaOH), sulfuric acid (H_2SO_4), and hydrogen chloride (HCl).

Extraction of silica from beach sand

Lhok Mee beach sand that had been pulverized was combined with 100 mL of 7.1 M hydrochloric acid (HCl) and stirred for 2 hours. After the filtrate was removed, the sand was washed in distilled water until the pH was near to neutral, and then dried for 2 hours at 110°C. A mixture was prepared by combining 60 g of sand with 80 g of NaOH. Subsequently, 50 mL of distilled water was gradually added to the mixture under continuous stirring until a thick consistency was achieved. The filtrate was transferred to a beaker, and 25 mL of H_2SO_4 was added cautiously, drop by drop. After being filtered, the resulting silica was heated to 180°C for 1.5 hours and then crushed into a powder.

Magnetite and composite preparation

The sand sample from Leungah was washed or rinsed until clean, then dried using an oven at 100°C for 5 hours. After drying, the iron sand contained in Leungah beach sand was separated using a magnetic rod until 30 g of iron sand was obtained. The 30 g of iron sand was mixed with 80 mL of concentrated hydrochloric acid (HCl 37%) while stirring for 30 minutes. After the iron sand dissolved, 40 mL of the solution was taken, and then 40 mL of 7 M sodium hydroxide (NaOH) solution was added dropwise while stirring until the pH reached 12. The appearance of a black precipitate indicated the formation of magnetite. The magnetite was washed with distilled water, filtered, and then heated in an oven at 80°C for 3 hours. For the preparation of silica magnetite composite, about 2 g silica was mixed to the iron solution before adding the NaOH solution. Finally, the magnetite and obtained composites are finely ground to obtain solid powders.

Material characterization

The molecular structure of the prepared materials was analyzed using a Shimadzu Fourier Transform-Infrared 8400 spectrophotometer (Perkin Elmer Spectrum One, Massachusetts, USA) from 500 cm^{-1} to 4,000 cm^{-1}. Prior to analysis, the materials were oven-dried at 40°C overnight and then ground together with KBr. Regarding the crystal structure analysis, a Shimadzu XRD-700 Series X-Ray Diffractometer from Kyoto, Japan was utilized. The samples were scanned at a rate of 8°/min using CuKα radiation (30 mA; 40 kV) within the range of 10° to 80° (2θ). Subsequently, morphology analyses were conducted on the sample surfaces through scanning electron microscopy and energy-dispersive X-ray spectroscopy (SEM-EDS), employing a Jeol JSM-6510 LA instrument from Tokyo, Japan. The observations were made at 500x magnification and operated at 15 kV.

Tetracycline adsorption

Each adsorbent (silica, magnetite, and composite) was accurately weighed to 0.02 g and placed into an Erlenmeyer flask containing 10 mL of a tetracycline solution. The adsorption performance was then systematically examined by varying the contact time (ranging from 0.5 to 24 hours), the adsorbent dosage (from 0.02 to 1.0 g), and subsequently, the initial tetracycline concentration (varying from 10 to 100 mg/L). The residual concentration of tetracycline was assessed by employing a UV–Vis spectrophotometer (UVmini-1240, Kyoto, Japan) at maximum wavelength (λ_{max}) = 357 nm. The calculation of the adsorption capacity at different time intervals (q_t, mg/g) and at equilibrium (q_e, mg/g) was carried out using the following equations:

$$q_t = \frac{(C_0 - C_t) \times V}{m} \tag{1}$$

$$q_e = \frac{(C_0 - C_e) \times V}{m} \tag{2}$$

where: C_0 – represents the initial concentration (mg/L), C_t stands for the concentration at time 't' (mg/L), C_e – denotes the concentration at equilibrium (mg/L), m – represents the weight of the adsorbent (g), V – the volume of the adsorbate (L).

To examine the adsorption kinetic of tetracyclines onto the adsorbents, the data were analyzed using the pseudo-first-order, pseudo-second-order, and Elovich models, as presented in Eqs. 3, 4, and 5 below:

$$q_t = q_e \left[1 - \exp(-k_1 t) \right] \tag{3}$$

$$q_t = \frac{k_2 q_e^2 t}{1 + k_2 q_e t} \tag{4}$$

$$q_t = \frac{1}{\beta} \ln(1 + \alpha \beta t) \tag{5}$$

where: k_1 – represents the rate constant of the pseudo-first-order model, k_2 – the rate

constant of the pseudo-second-order model, while ,α' and ,β' are the Elovich constants.

By utilizing the optimal adsorption condition determined in the assessment of contact time and adsorbent dosage, isotherm studies were conducted over a range of initial tetracycline concentrations from 10 to 80 mg/L. The adsorption isotherm was predicted using non-linear equations of the Langmuir model (Eq. 6) and the Freundlich model (Eq. 7).

$$q_e = \frac{q_{max}\, b\, C_e}{(1 + b\, C_e)} \tag{6}$$

$$q_e = K_F\, C_e^{1/n} \tag{7}$$

where: q_{max} – represents the maximum adsorption capacity (mmol/kg), b – serves as a measure of the energy of adsorption, K_F – stands for the Freundlich adsorption constant, n – associated with the adsorption intensity.

RESULT AND DISCUSSION

This research utilized beach sand samples from two different coastal locations. The samples were collected from Lhok Mee Beach and Leungah Beach due to their distinct characteristics.

Physically, the Lhok Mee Beach sand has a whiter color compared to the Leungah Beach sand. This variation is influenced by the mineral composition present within them. According to Saniah et al. (2014), the Lhok Mee Beach sand contains a higher concentration of silica (SiO_2) with a homogeneous layer structure, resulting in a white coloration. The significant presence of silica leads to the sandy shoreline appearing white, hence the name "White Sand Beach" for Lhok Mee Beach. In contrast, Leungah Beach sand is predominantly composed of the Fe_3O_4 mineral, giving it a darker coloration with a heterogeneous layer structure. The upper layer is deep black, while the lower layer is grayish. Due to the prevalence of black iron oxide minerals in the Leungah Beach sand, it is often referred to as "iron sand" or "magnetite sand." Consequently, in this study, silica is extracted from the Lhok Mee Beach sand, while magnetite is extracted from the Leungah Beach sand.

Adsorbent characteristics

The results of characterizing silica, magnetite, and silica-magnetite composite using XRD are shown in Figure 1. As it can be observed, the diffractogram of silica extracted from the Lhok Mee Beach sand exhibits a broad peak located within the 2θ range of 15°–30°, centered between 22° and 23° with low intensity, indicating that the
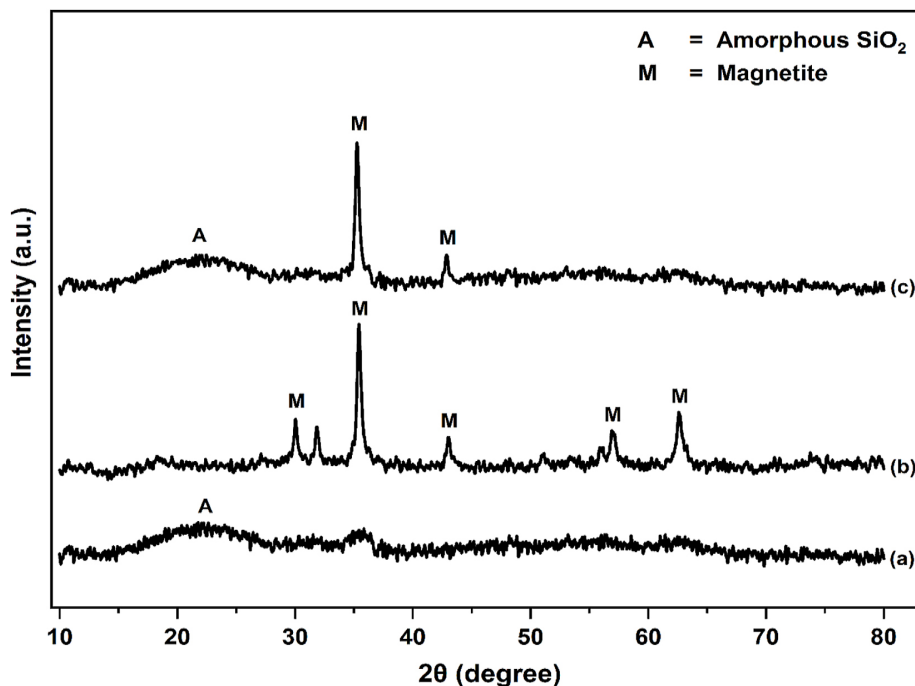

Fig. 1. Diffractograms of (a) silica, (b) magnetite, and (c) silica-magnetite composite

resulting silica is in an amorphous state. The shift of the peak towards lower 2θ angles is attributed to the increased sodium hydroxide content. Furthermore, the absence of other peaks correlates with the purity of the obtained silica (Boualem et al., 2022). In the diffractogram of magnetite extracted from Leungah Beach sand, there are five distinct and strong peaks of magnetite observed at 2θ angles (d values) of 30.03° (2.97), 35.43° (2.53), 43.04° (2.09), 56.97° (1.61), and 62.63° (1.48). The appearance of these peaks indicates the formation of magnetite, consistent with the findings reported by Ouyang et al. (2015). This is also evidenced by the strong attraction between magnetite powder and a magnetic rod when they are in close proximity. In the diffractogram of the silica-magnetite composite, there is a broad peak in the 2θ range of 15°–30°, representing the amorphous silica, as well as two distinctive magnetite peaks at 35.43° (2.53) and 43.04° (2.09). The presence of these peaks confirms the successful formation of the silica-magnetite composite. To further support this argument, additional characterization was conducted using FTIR.

Figure 2 displays FTIR spectra of silica, magnetite, and silica-magnetite composite. The FTIR spectrum of silica extracted from the Lhok Mee Beach sand reveals several distinct bands, located at 459 cm⁻¹, 686 cm⁻¹, 1085 cm⁻¹, 1,642 cm⁻¹, and 3,468 cm⁻¹. The band appearing at 3,468 cm⁻¹ signifies the stretching vibration of -OH groups. The presence of the sharp and dominant absorption peak at 1,085 cm⁻¹ indicates the asymmetric stretching of the Si-O-Si bonds (siloxane). The vibrational stretching of the Si-OH bonds (silanol), as confirmed by the peak at 686 cm⁻¹, suggests the amorphous structure of SiO_2. The stretching of the O-Si-O bonds (siloxy) is marked by the absorption peak at 459 cm⁻¹. The IR band at 1,642 cm⁻¹ is attributed to the bending vibration of H-O-H from water molecules that did not evaporate during the drying process. Trapped water within the silica structure often leads to the appearance of the Si-OH bands formed by intermolecular hydrogen bonding. Meanwhile, in the FTIR spectrum of magnetite, the presence of the Fe-O functional groups is observed at wave numbers of 445 cm⁻¹ and 579 cm⁻¹. Consistent with the findings of Silva et al. (2020), the characteristic vibrations of the Fe–O bonds in magnetite appear in the range of approximately 425 cm⁻¹ to 624 cm⁻¹. In the silica-magnetite composite, the formation of magnetite, as indicated by the Fe-O absorption peak, causes the Si-O absorption peak to shift to lower wave numbers.

Figure 3 shows the SEM results of silica, magnetite, and the silica-magnetite composite. On the basis of these results, the produced silica appears in agglomerated form (Figure 3a). This form is attributed to the drying technique used
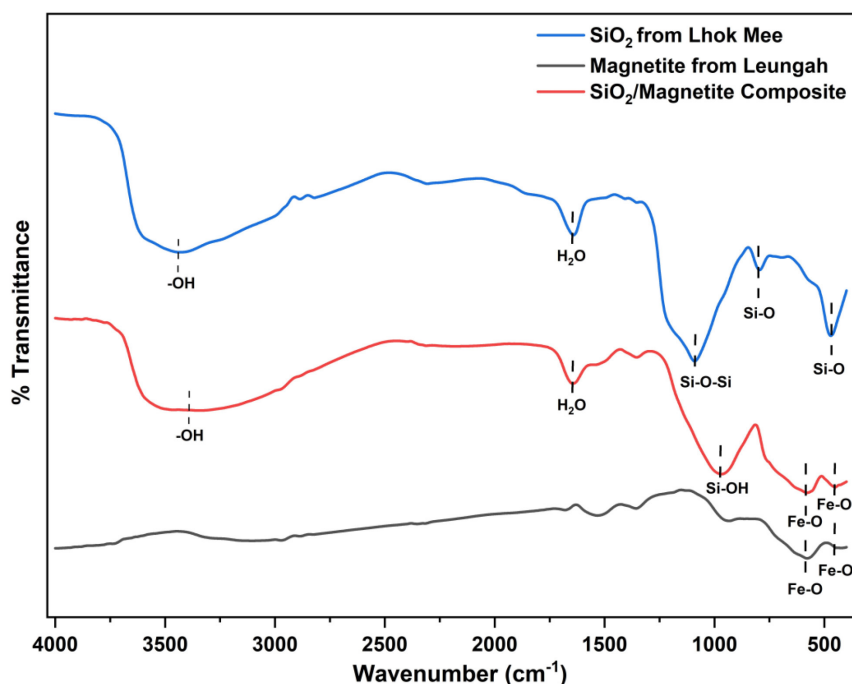

Fig. 2. FTIR spectra of silica, magnetite, and silica-magnetite composite

(thermal drying), where excessive agglomeration is known to occur compared to alcohol dehydration (Boualem et al., 2022). The morphology of magnetite particles (Figure 3b) exhibits irregular distribution. It is known that the growth of magnetite particles is influenced by their isotropic unit cell structure, allowing them to take on various shapes, both spherical and non-spherical. Variations in particle size, size distribution, and shape can significantly alter material properties. Similarly, optoelectronic characteristics involving charge transfer, concentration, mobility, and conductivity are highly dependent on these factors. Small variations in size and shape can lead to significant improvements in the mentioned factors. Magnetite particles have an inverse spinel cubic structure and they have a strong tendency to form aggregates due to their high surface energy and strong magnetic dipole-dipole interactions. Meanwhile, the silica-magnetite composite exhibits a combined morphological form of both silica and magnetite, with silica being interspersed within magnetite (Figure 3c).
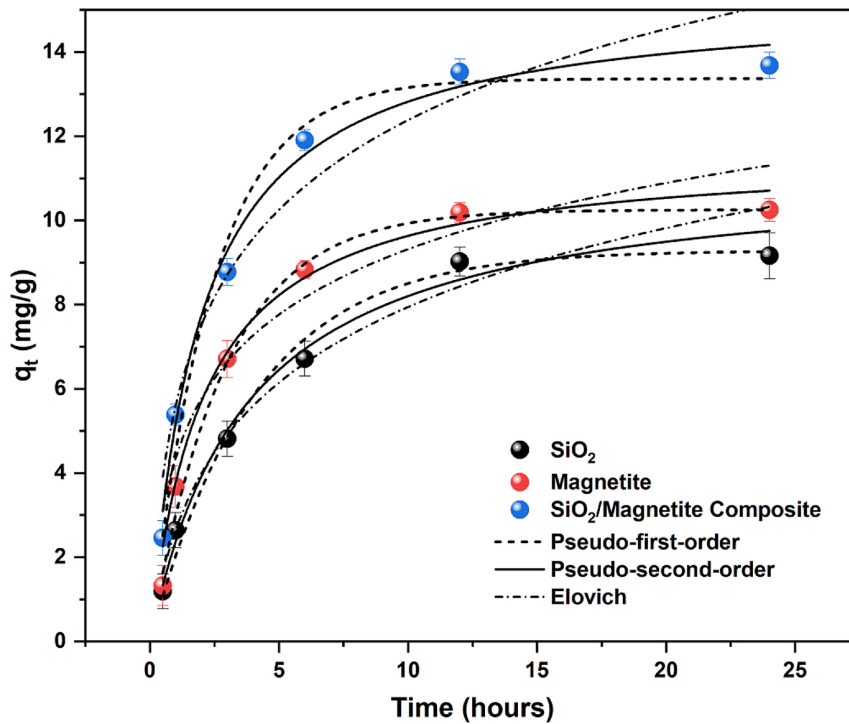
Tetracycline adsorption kinetics onto adsorbents

Figure 4 depicts the influence of time on tetracycline adsorption from 0.5 hours to 24 hours. The results indicate that with longer duration (ranging from 0.5 to 12 hours), the tetracycline adsorption capacity increases, whether using silica, magnetite, or the composite adsorbent. The increase in adsorption capacity with extended contact time can be explained by several key factors. Firstly, as the contact time increases, more opportunities for the molecules of the substance to be adsorbed to interact with the surface of the adsorbent material. This implies that more molecules can be adsorbed onto the surface of the material, subsequently enhancing the adsorption capacity. Additionally, an extended contact time allows the adsorption process to reach equilibrium. This occurs between 12 hours and 24 hours, with adsorption capacities of 9.16±0.55 mg/g (silica), 10.24±0.26 mg/g (magnetite), and 13.68±0.31 mg/g (composite) at the 24-hour adsorption time. Therefore, a 24-hour contact time was chosen to maximize the tetracycline adsorption process. The calculated parameters and correlation results are presented in Table 1. The correlation coefficients indicate that three
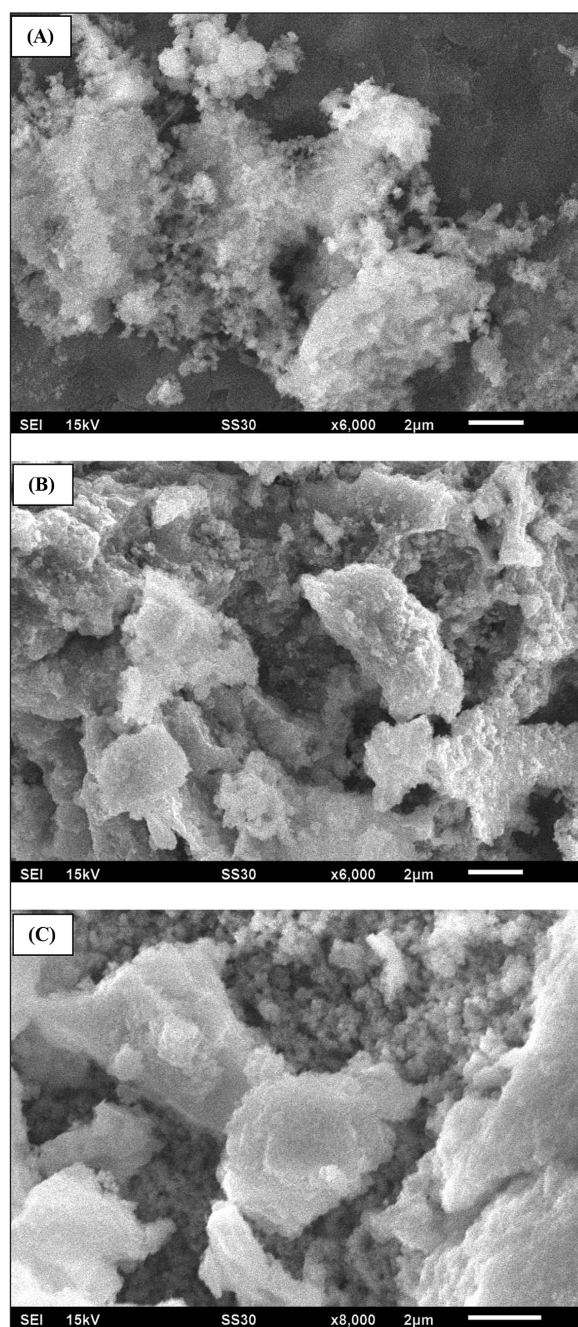
Fig. 3. Morphology of (a) silica, (b) magnetite, and (c) composite

models are in good agreement with the tetracycline adsorption process on the sorbents. In comparison to the pseudo-second-order and Elovich models, the pseudo-first-order model exhibited higher correlation coefficients ($R_2 > 0.99$). The experimental and calculated values of q_e were in close agreement, suggesting that the pseudo-first-order model is a more suitable description of the tetracycline sorption progress on the sorbents. Previous studies conducted by Miao et al. (2019) and Foroutan et al.

Fig. 4. Adsorption kinetics of tetracycline onto silica, magnetite and composite. Experimental conditions: tetracycline concentration = 50 mg/L, m = 0.02 g, pH = 6.8±0.1, T = 30°C

(2021), employing other adsorbents, have also shown that the adsorption of tetracycline follows a pseudo-first-order model.

Effect of adsorbent dosage

Figure 5 illustrates the influence of adsorbent weight on tetracycline adsorption over 24 hours. The results show that as the percentage of tetracycline adsorption increases along with adsorbent weight, whether using silica, magnetite, or the composite. When 0.02 g of adsorbent was used, the percentage of tetracycline adsorption using silica, magnetite, and the composite was 27.23%, 41.35%, and 54.74%, respectively. However, the difference in tetracycline adsorption percentage between 0.02 g and 0.1 g of adsorbent was not very significant. Therefore, the use of 0.02 g of adsorbent is preferred to minimize the amount of adsorbent used in the adsorption process.

Table 1. Non-linear form of kinetic model parameters for the removal of tetracyclines

| Kinetic models	Parameters	Values		
		SiO_2	Magnetite	SiO_2/Magnetite
Pseudo-first-order	q_e (mg/g)	9.285±0.372	10.253±0.163	13.367±0.463
	k_1 (min^{-1})	0.247±0.029	0.346±0.024	0.415±0.050
	R^2	0.987	0.993	0.991
	RMSE	0.986	0.861	2.276
Pseudo-second-order	q_e (mg/g)	11.264±0.626	11.63±0.462	15.324±0.51
	k_2 (g/(mg.min))	0.023±0.005	0.041±0.009	0.033±0.005
	R^2	0.988	0.979	0.988
	RMSE	0.975	1.509	1.693
Elovich	α (mg/(g.min))	4.397±1.246	13.00±9.018	15.438±6.556
	β (g/mg)	0.353±0.054	0.434±0.098	0.315±0.051
	R^2	0.972	0.897	0.9433
	RMSE	1.475	3.346	3.811
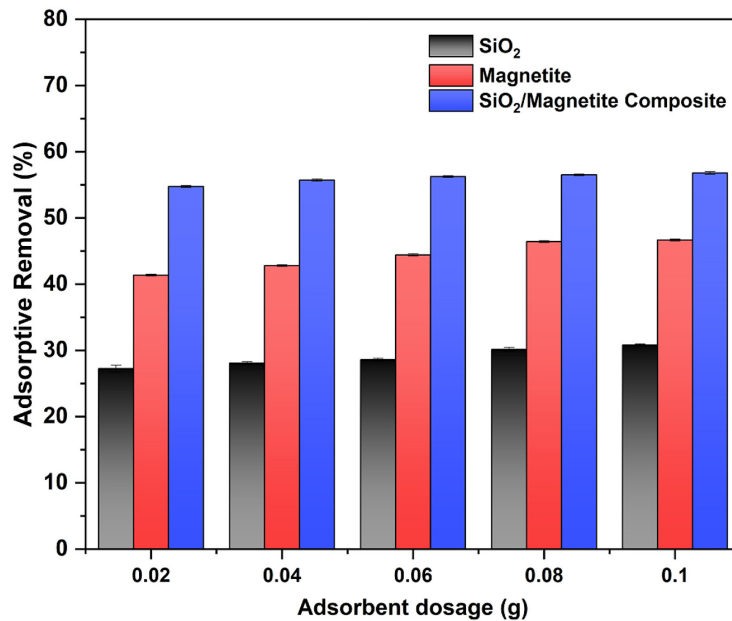
Fig. 5. Effect of adsorbent dosage for the removal of tetracycline. Experimental conditions: tetracycline concentration = 50 mg/L, t = 24 h, pH = 6.8±0.18, T = 30°C

Adsorption isotherms of tetracyclines onto adsorbents

Adsorption isotherms serve as valuable tools for explaining the distribution of adsorbate molecules between the liquid and solid phases at equilibrium, offering insights into the interactions between the adsorbent and adsorbate. In this study, the experimental data was fitted to the Langmuir and Freundlich isotherm models. The non-linear adjustments of

these models are illustrated in Figure 6, and the corresponding parameter values are provided in Table 2. The Langmuir model characterizes an adsorption process occurring on a homogeneous surface with the adsorbate forming monolayers. According to Table 2, the Langmuir model yielded a determination coefficient (R_2) of 0.958 (silica), 0.993 (magnetite), and 0.954 (composite). Another crucial parameter, the separation factor (b), was used to evaluate the favorability of the adsorption process: 0 < b <
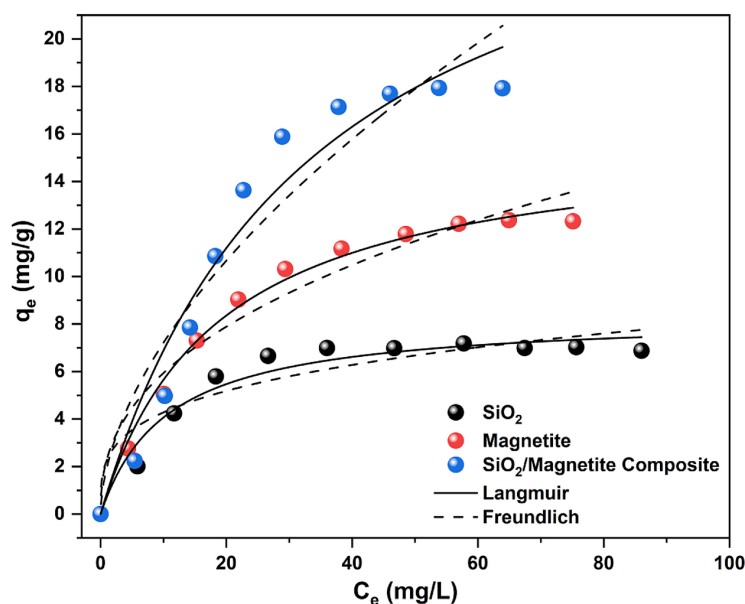

Fig. 6. Adsorption isotherms of tetracyclines onto silica, magnetite and composite. Experimental conditions: m = 0.02 g, t = 24 h, pH = 6.8±0.21, T = 30°C

Table 2. Non-linear form of adsorption isotherm model parameters

Isotherm models	Parameters	Value		
		SiO_2	Magnetite	SiO_2/Magnetite
Langmuir	q_{max} (mg/g)	8.36±0.448	16.055±0.511	29.955±4.165
	b (L/mg)	0.094±0.021	0.054±0.005	0.029±0.008
	R^2	0.958	0.993	0.954
	RMSE	0.524	0.373	1.505
Freundlich	k_F (mg/g)	2.267±0.568	2.308±0.423	1.966±0.649
	n (g/mg.min))	3.623±0.857	2.438±0.289	1.771±0.284
	R^2	0.887	0.958	0.914
	RMSE	0.858	0.917	2.069

1 for favorable, b > 1 for unfavorable, and b = 0 for irreversible adsorption. The b values in this study ranged from 2.9×10^{-2} to 9.4×10^{-2}, indicating that the adsorption of tetracyclines onto silica, magnetite, and composite adsorbents is favorable within the studied concentration range. The Freundlich model is an empirical equation based on adsorption occurring on a heterogeneous surface with sites of varying affinities. As seen in Table 2, the Freundlich model achieved an R^2 of 0.887 (silica), 0.958 (magnetite), and 0.914 (composite). The n parameter, often referred to as the heterogeneity factor, is used to determine whether the adsorption process is physical (n > 1), chemical (n < 1), or linear (n = 1). In the case of the composite, the n value was 1.771±0.284, indicating that the physical process is favorable. The 1/n ratio provides insights into the heterogeneity of the surface, where a value closer to zero indicates a more heterogeneous surface. For the SM composite, the 1/n value was 0.564, signifying a degree of surface heterogeneity. In comparison to the Freundlich model, the Langmuir isotherm was found to be a better fit for describing the adsorption process, indicating that the adsorption occurred in a single-molecule layer. The maximum adsorption capacity (q_{max}) of the adsorbents ranked as composite (29.955±4.165) > magnetite (16.055±0.511) > silica (8.36±0.448).

CONCLUSIONS

Silica-magnetite composite has been successfully synthesized using silica and magnetite particles extracted from local beach sand through the co-precipitation method. The formation of SM composites was confirmed via various characterizations, including Fourier-transform infrared spectroscopy, X-ray diffraction, and scanning electron microscope analysis. The pseudo-first-order kinetic model, with high correlation coefficients ($R^2 > 0.99$) exceeding those of the pseudo-second-order and Elovich models, was found to be the most suitable kinetic model. In terms of adsorption isotherms, the non-linear Langmuir model provided the best fit ($R^2 = 0.954$) with a root-mean-square error of 1.505, outperforming the Freundlich model. This confirms that the mechanism of tetracycline adsorption onto SM composites is mainly attributed to electrostatic interactions and hydrogen bonding. The maximum adsorption capacity of tetracycline on the SM composite reached 29.955±4.165 mg/g at a 24-hour contact time, with an adsorption rate constant of 0.415±0.050 min^{-1}. The environmentally friendly composite prepared in this research exhibits promising potential as an effective adsorbent with good tetracycline removal capabilities. The effectiveness needs to be further investigated to evaluate their impact on pH variations and their potential for reusing in the removal of tetracycline, enabling their sustainable application in large-scale aquatic industries.

Acknowledgements

REFERENCES

1. Amaly, N., EL-Moghazy, A.Y., Nitin, N., Sun, G., Pandey, P.K. 2022. Synergistic adsorption-photocatalytic degradation of tetracycline by microcrystalline cellulose composite aerogel dopped with

montmorillonite hosted methylene blue. Chemical Engineering Journal, 430, 133077.

2. Behrami, E., Xhaxhiu, K., Dragusha, B., Reka, A., Andoni, A., Hamiti, X., Drushku, S. 2022. The Removal of Atrazine and Benalaxyl by the Fly Ash Released from Kosovo A Power Plant. International Journal of Analytical Chemistry, 2022.

3. Boualem, A., Leontie, L., Lopera, S.A.G., Hamzaoui, S. 2022. Synthesis and Characterization of Mesoporous Silica from Algerian River Sand for Solar Grade Silicon: Effect of Alkaline Concentration on the Porosity and Purity of Silica Powder. Silicon, 1-10.

4. Chang, D., Mao, Y., Qiu, W., Wu, Y., Cai, B. 2023. The Source and Distribution of Tetracycline Antibiotics in China: A Review. Toxics, 11(3), 214.

5. Chapkanski, S., Brocard, G., Lavigne, F., Meilianda, E., Ismail, N., Darusman, D., Goiran, J.P. 2022. Fingerprinting sources of beach sands by grain-size, using mid-infrared spectroscopy (MIRS) and portable XRF. Implications for coastal recovery along a tsunami-struck delta coastline. Catena, 219, 106639.

6. De Mastro, F., Cacace, C., Traversa, A., Pallara, M., Cocozza, C., Mottola, F., Brunetti, G. 2022. Influence of chemical and mineralogical soil properties on the adsorption of sulfamethoxazole and diclofenac in Mediterranean soils. Chemical and Biological Technologies in Agriculture, 9(1), 34.

7. Ewis, D., Ba-Abbad, M.M., Benamor, A., El-Naas, M.H. 2022. Adsorption of organic water pollutants by clays and clay minerals composites: A comprehensive review. Applied Clay Science, 229, 106686.

8. Foroutan, R., Peighambardoust, S.J., Latifi, P., Ahmadi, A., Alizadeh, M., Ramavandi, B. 2021. Carbon nanotubes/β-cyclodextrin/MnFe2O4 as a magnetic nanocomposite powder for tetracycline antibiotic decontamination from different aqueous environments. Journal of Environmental Chemical Engineering, 9(6), 106344.

9. Ghosh, N., Sen, S., Biswas, G., Saxena, A., Haldar, P.K. 2023. Adsorption and desorption study of reusable magnetic iron oxide nanoparticles modified with Justicia adhatoda leaf extract for the removal of textile dye and antibiotic. Water, Air, & Soil Pollution, 234(3), 202.

10. Kumaravel, M.S., Alagumurthi, N., Mathiyalagan, P. 2022. Energy Optimization Using Silicon Dioxide Composite and Analysis of Wire Electrical Discharge Machining Characteristics. Hybrid Intelligent Approaches for Smart Energy: Practical Applications, 67-82.

11. Le, V.V., Tran, Q.G., Ko, S.R., Lee, S.A., Oh, H.M., Kim, H.S., Ahn, C.Y. 2023. How do freshwater microalgae and cyanobacteria respond to antibiotics?. Critical Reviews in Biotechnology, 43(2), 191-211.

12. Li, S., Ondon, B.S., Ho, S.H., Zhou, Q., Li, F. 2023. Drinking water sources as hotspots of antibiotic-resistant bacteria (ARB) and antibiotic resistance genes (ARGs): Occurrence, spread, and mitigation strategies. Journal of Water Process Engineering, 53, 103907.

13. Miao, J., Wang, F., Chen, Y., Zhu, Y., Zhou, Y., Zhang, S. 2019. The adsorption performance of tetracyclines on magnetic graphene oxide: A novel antibiotics absorbent. Applied Surface Science, 475, 549-558.

14. Ouyang, Z.W., Chen, E.C., Wu, T.M. 2015. Thermal stability and magnetic properties of polyvinylidene fluoride/magnetite nanocomposites. Materials, 8(7), 4553-4564.

15. Prajaputra, V., Isnaini, N. 2023. Assessment of Metformin Stability and Its Removal from Water by Pumice-Based Zeolite. Jurnal Penelitian Pendidikan IPA, 9(7), 4909-4916.

16. Prajaputra, V., Abidin, Z., Budiarti, S., Suryaningtyas, D.T., Isnaini, N. 2021. Comparative study of methylene blue adsorption using alkali-activated pumice from Bali and Banten. Journal of Physics: Conference Series, 1882(1), 012118.

17. Prajaputra, V., Abidin, Z., Suryaningtyas, D.T., Rizal, H. 2019. Characterization of Na-P1 zeolite synthesized from pumice as low-cost materials and its ability for methylene blue adsorption. IOP Conference Series: Earth and Environmental Science, 399(1), 012014.

18. Prasetya, N., Wenten, I.G., Franzreb, M., Wöll, C. 2023. Metal-organic frameworks for the adsorptive removal of pharmaceutically active compounds (PhACs): Comparison to activated carbon. Coordination Chemistry Reviews, 475, 214877.

19. Qiu, H., Ni, W., Yang, L., Zhang, Q. 2022. Remarkable ability of Pb (II) capture from water by self-assembled metal-phenolic networks prepared with tannic acid and ferric ions. Chemical Engineering Journal, 450, 138161.

20. Rajeev, R., Adithya, K.K., Kiran, G.S., Selvin, J. 2021. Healthy microbiome: a key to successful and sustainable shrimp aquaculture. Reviews in Aquaculture, 13(1), 238-258.

21. Rigos, G., Kogiannou, D., Padrós, F., Cristofol, C., Florio, D., Fioravanti, M., Zarza, C. 2021. Best therapeutic practices for the use of antibacterial agents in finfish aquaculture: A particular view on European seabass (Dicentrarchus labrax) and gilthead seabream (Sparus aurata) in Mediterranean aquaculture. Reviews in aquaculture, 13(3), 1285-1323.

22. Said, H.A., Noukrati, H., Mahdi, I., Oudadesse, H., Barroug, A. 2023. In situ precipitated hydroxyapatite-chitosan composite loaded with ciprofloxacin: Formulation, mechanical, in vitro antibiotic uptake, release, and antibacterial properties. Materials Chemistry and Physics, 294, 127008.

23. Salma, U., Shafiujjaman, M., Al Zahid, M., Faruque, M.H., Habibullah-Al-Mamun, M., Hossain,

A. 2022. Widespread Use of Antibiotics, Pesticides, and Other Aqua-Chemicals in Finfish Aquaculture in Rajshahi District of Bangladesh. Sustainability, 14(24), 17038.

24. Saniah, S., Purnawan, S., Karina, S. 2014. Karakteristik dan kandungan mineral pasir pantai Lhok Mee, Beureunut dan Leungah, Kabupaten Aceh Besar. Depik, 3(3).

25. Sarker, P., Lei, X., Taylor, K., Holmes, W., Yan, H., Cao, D., Zappi, M.E., Gang, D.D. 2023. Evaluation of the adsorption of sulfamethoxazole (SMX) within aqueous influents onto customized ordered mesoporous carbon (OMC) adsorbents: Performance and elucidation of key adsorption mechanisms. Chemical Engineering Journal, 454, 140082.

26. Saxena, R., Saxena, M., Lochab, A. 2020. Recent progress in nanomaterials for adsorptive removal of organic contaminants from wastewater. Chemistry Select, 5(1), 335-353.

27. Silva, C.A., Silva, R.L., Figueiredo, A.T.D., Alves, V.N. 2020. Magnetic solid-phase microextraction for lead detection in aqueous samples using magnetite nanoparticles. Journal of the Brazilian Chemical Society, 31, 109-115.

28. Yun, X., Zhou, J., Wang, J., Li, Q., Wang, Y., Zhang, W., Fan, Z. 2023. Biological toxicity effects of florfenicol on antioxidant, immunity and intestinal flora of zebrafish (Danio rerio). Ecotoxicology and Environmental Safety, 265, 115520.

29. Zeidman, A.B., Rodriguez-Narvaez, O.M., Moon, J., Bandala, E.R. 2020. Removal of antibiotics in aqueous phase using silica-based immobilized nanomaterials: A review. Environmental Technology & Innovation, 20, 101030.